Journal of Advanced Research (2015) 6, 563–569

Cairo University

Journal of Advanced Research

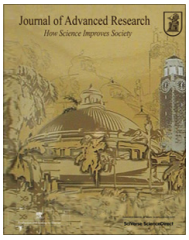

ORIGINAL ARTICLE

The role of $MgBr_2$ to enhance the ionic conductivity of PVA/PEDOT:PSS polymer composite

Eslam M. Sheha *, Mona M. Nasr, Mabrouk K. El-Mansy

Physics Department, Faculty of Science, Benha University, Benha 13518, Egypt

ARTICLE INFO

Article history:
Received 10 September 2013
Received in revised form 11 January 2014
Accepted 22 January 2014
Available online 1 February 2014

Keywords:
Polymer electrolyte
Ionic conductivity
Magnesium ion conductor
PVA

ABSTRACT

A solid polymer electrolyte system based on poly(vinyl alcohol) (PVA) and poly(3,4-Etylenedioxythiophene):poly(styrenesulfonate) (PEDOT:PSS) complexed with magnesium bromide ($MgBr_2$) salt was prepared using solution cast technique. The ionic conductivity is observed to increase with increasing $MgBr_2$ concentration. The maximum conductivity was found to be 9.89×10^{-6} S/cm for optimum polymer composite film (30 wt.% $MgBr_2$) at room temperature. The increase in the conductivity is attributed to the increase in the number of ions as the salt concentration is increased. This has been proven by dielectric studies. The increase in conductivity is also attributable to the increase in the fraction of amorphous region in the electrolyte films as confirmed by their structural, thermal, electrical and optical properties.

Introduction

Electrolytes are ion conducting materials formed by dissolving ions in a host substance. They are used in a multitude of electrochemical devices such as batteries, fuel cells, super capacitors, and electrochromic smart windows [1–5]. Blending of polymers is an economical technique to develop new polymeric materials with properties that are superior, intermediate, or just different from those of individual component polymers, it has been reported that the polymer electrolytes developed using polymer blends exhibited higher conductivity. The enhancement of conductivity has been attributed to the increase in amorphous region in the blend based electrolytes [6]. These polymers have been complexed with various salts to provide the ions for conduction [7].

PVA has excellent film forming, emulsifying, and adhesive properties. It is also resistant to oil, grease and solvent. It is odorless and nontoxic. It has high tensile strength and flexibility, as well as high oxygen and aroma barrier properties. However these properties are dependent on humidity, in other words, with higher humidity more water is absorbed. PVA is fully degradable and is a quick dissolver. PVA has a melting point of 230 °C and 180–190 °C for the fully hydrolyzed and partially hydrolyzed grades, respectively. It decomposes rapidly above 200 °C as it can undergo pyrolysis at high temperatures [8].

* Corresponding author. Tel.: +20 1007414705; fax: +20 133222578.
E-mail addresses: e_sheha@yahoo.com, ISLAM.SHIHAH@fsc.bu.edu.eg (E.M. Sheha).

Peer review under responsibility of Cairo University.

2090-1232 © 2014 Production and hosting by Elsevier B.V. on behalf of Cairo University.
http://dx.doi.org/10.1016/j.jare.2014.01.010

PEDOT:PSS is one of the most promising conducting polymers for industrial applications [9–11]. PEDOT:PSS has attracted considerable attention because of its superior electrical and good thermal stability, it could be used in organic devices as a hole transport layer (HTL) and has the potential to substitute for metal electrodes due to its high conductivity [12–16]. It is a bio-compatible, easily processed and non-toxic material, which is widely used in electronic, optical, electrochemical and biomedical applications [17,18]. Other advantages of PEDOT:PSS such as high transparency in the visible range, long-term stability, and solution processability [19]. Earlier studies in PEDOT:PSS indicated that the enhancement in conductivity is due to screening effect of the solvents, increased hopping transport, improved connectivity among conducting grains, etc. [20–23].

Magnesium bromide ($MgBr_2$) is the fast conducting salt in a number of crystalline and amorphous materials, its incorporation in a polymeric system may be expected to enhance its electrical performance.

PVA/PEDOT:PSS (PVPS) has been developed to obtain high conductivity equal to 2.79×10^{-7} S/cm for the optimum concentration 1.6 wt.% [24]. This PVPS blend has been considered to get PVPS/$MgBr_2$ by adding $MgBr_2$ nanoparticles to optimize polymer electrolyte membrane through studying its structural, thermal, electrical and optical properties.

Experimental

PVA (98–99% hydrolyzed, Alfa Aesar, average M.W. 88,000–97,000), PEDOT:PSS (solid concentration 1.2% and conductivity = 1 S/cm), $MgBr_2$ were received from Sigma. The solution casting method that is used to prepare the PVPS samples could be found in Ref. [24]. The complex electrolytes were prepared by mixing PVPS with $MgBr_2$ at several ratios in distilled water to get $(PVPS)_{1-x'}(MgBr_2)_{x'}$ complex electrolytes (x' = 0, 10, 20, 30 wt.%). The mixture was then poured into Petri dishes and left to dry for four weeks in dry atmospher.

X-ray diffraction has been accomplished to investigate composite samples crystallinity using SHIMADZU diffractometer type XRD 6000. The diffraction system based with Cu tube anode with voltage 40 kV, current 30 mA & wavelength $K_{\alpha 1}$ = 1.5418 Å. The start angle (2θ) was 5° and the end angle was 70°. Bragg's Law ($n\lambda = 2d\sin\theta$) was used to compute the crystallographic spacing. The surface morphology of these polymer electrolytes was examined by scanning electron microscopy (SEM, JOEL-JSM Model 5600). Thermogravimetric analysis were carried out by using Shimadzu thermal analyzer with heating rate 10 °C/min, under N_2 (20 ml/min) flow in the range up to 0–400 °C. AC measurements were carried out in the temperature range 303–373 K using PM 6304 programmable automatic RCL (Philips) meter. The measurements were carried out over a frequency range 100 *Hz* to 100 k*Hz*. The absorption spectra of the PVPS/$MgBr_2$ colloidal were recorded in the wavelength range (400–1100 nm) using a UV–VIS spectrophotometer (PG, T80$^+$).

Results and discussion

Fig. 1 shows XRD patterns of $(PVPS)_{1-x'}(MgBr_2)_{x'}$ polymer composite. It is clear from the figure that the pure PVA shows the presence of a semi-crystalline phase with the characteristic diffraction peak located at 19.4°. This peak becomes less intense and more broadening as the $MgBr_2$ content is increased due to transference of PVA from semicrystalline to amorphous structure. This is in agreement with previously obtained data [25].

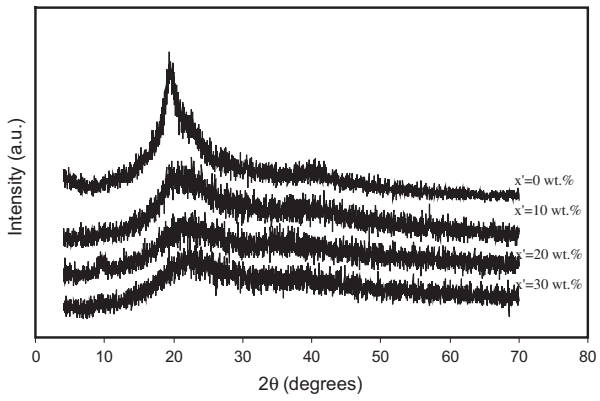

Fig. 1 XRD patterns of $(PVPS)_{1-x'}(MgBr_2)_{x'}$ polymer composites.

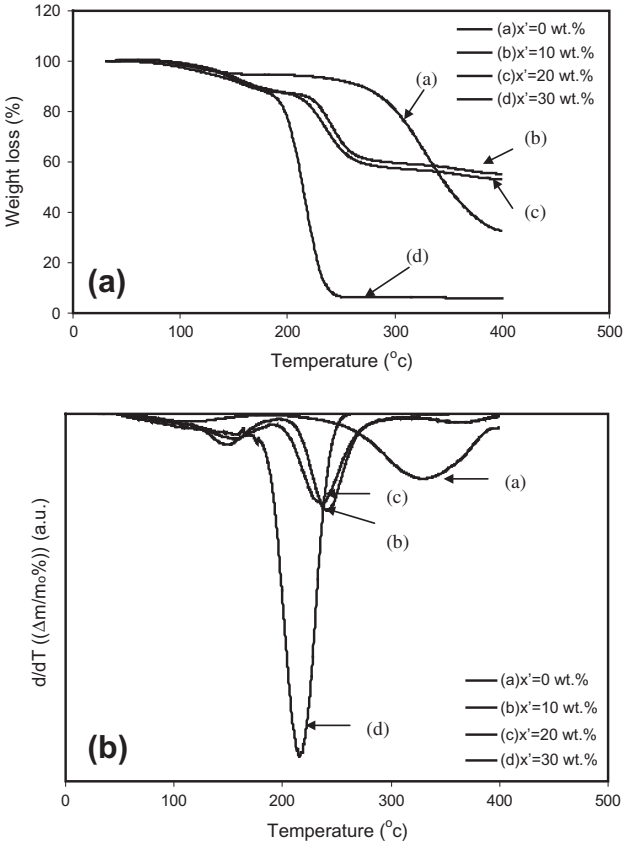

Fig. 2 Thermal analysis, (a) TGA thermograms and (b) differential TGA, for $(PVPS)_{1-x'}(MgBr_2)_{x'}$ polymer composites.

Fig. 2a shows the TGA curves for $(PVPS)_{1-x'}(MgBr_2)_{x'}$ polymer composite. It is clear that the weight loss of composite samples occurred in different ranges of temperature has been obtained and plotted in Fig. 2b. The first maximum weight loss appeared at T_p = 150 °C which can be attributed to the dehydration of the inorganic salt ($MgBr_2$) in the polymer composite

matrix where the bigger peak of weight loss appear in the range 218.5 and 333.4 °C which shifts to relatively temperature range with increasing $MgBr_2$ concentration. The weight loss in mentioned range of temperature can be attributed to the release of compound water in the composite matrix. The shift of such peak to lower temperature range can be attributed to the increase of matrix porosity which enhances the water release.

The activation energy for the thermal decomposition of the samples can be calculated using the first order integral equation of Coates and Redfern [26],

$$\log\left[\frac{-\log(1-\alpha)}{T^2}\right] = \log\frac{R}{\Delta E}\left[1-\frac{2RT}{E}\right] - \frac{E}{2.304RT} \quad (1)$$

where T is the absolute temperature, E is the activation energy in J/mol, R is the universal gas constant (8.3136 J/mol K), n is the order of reaction, and α is the fractional weight loss at that particular temperature is calculated as

$$\alpha = \frac{w_i - w_t}{w_i - w_f} \quad (2)$$

where w_i is the initial weight, w_t is the weight at given temperature and w_f is the final weight of the sample. By plotting $-\log\left[-\log(1-\alpha)/T^2\right]$ against $1000/T$ for each sample as shown in Fig. 3, we obtain straight lines. Then, the apparent activation energies are calculated from the slopes of these lines using the expression:

$$E = 2.303R \times slope \quad (3)$$

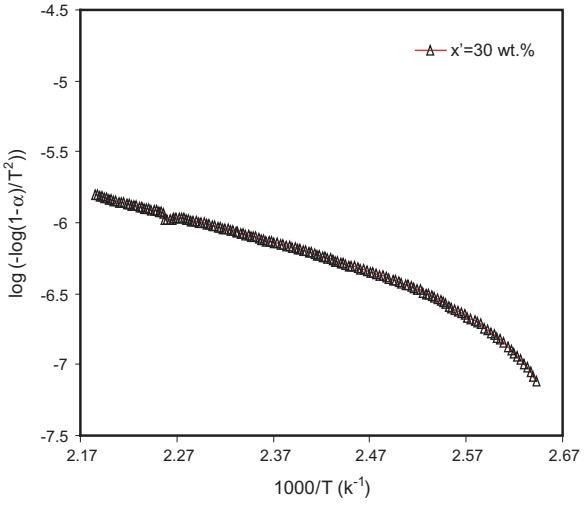

Fig. 3 Temperature dependence of weight loss fraction for $(PVPS)_{1-x'}(MgBr_2)_{x'}$ polymer composites.

Values of the apparent activation energy (E_a) of the samples are listed in Table 1. From this table, it is clear that the activation energy values lie in the range 132–189 kJ/mole which are less than the binding energy for the PVA/PEDOT:PSS essential bonds C—O, C=O, C≡O and H—O (=358, 799, 1072 and 459 kJ/mole respectively). Therefore the weight loss of the polymer composites can be attributed to compound water release. In addition the maximum weight loss temperature is shifted to lower temperature range which can be attributed to the moisture on salt release.

Fig. 4 shows SEM images of the $(PVPS)_{1-x'}(MgBr_2)_{x'}$ polymer composite. A comparison of the surface morphology shows marked changes by adding $MgBr_2$ to PVPS. The film at $x' = 10$ wt.% contains some tiny pores at surface morphology relative to pure PVPS.

Fig. 5a shows the complex impedance spectra of $(PVPS)_{1-x'}(MgBr_2)_{x'}$ polymer composite at 303 K. The complex plot shows semicircle does pass through the origin, and the equivalent circuit consisting of the parallel resistance (bulk resistance, R_b) and the capacitance (bulk capacitance, C_b) network showed in Fig. 5a (inset). Symbols Z' and Z'' refer to the real and imaginary components, respectively. The bulk resistance was used subsequently for evaluation the bulk conductivity,

$$\sigma_b = \frac{1}{R_b}(L/A) \quad (4)$$

where R_b is the bulk resistance, A is the cross sectional area of the sample and L is the thickness of the sample.

The extracted values of σ_b for the different $MgBr_2$ concentrations have been plotted versus the concentration, Fig. 5b. It is observed that bulk conductivity σ_b obeys the following relation:

$$\sigma_b = \sigma_o e^{\frac{C}{C_O}} \quad (5)$$

where σ_b is the bulk conductivity at $C = 0$ and C_O is a characteristic $MgBr_2$ concentrations. Both σ_o and C_O have been extracted using the least square fitting of Eq. (5) which is equal to 2.74×10^{-7} S/cm and 9.35 wt.%.

Fig. 6a shows the variation of the ac conductivity as a function of inverse temperature for $(PVPS)_{1-x'}(MgBr_2)_{x'}$ polymer composite at 1 kHz. This behavior follows Arrhenius relation:

$$\sigma = \sigma_o \exp\left(\frac{-E_a}{KT}\right) \quad (6)$$

where σ_o is the pre-exponential factor, E_a is activation energy, K is Boltzman constant and T is absolute temperature. As shown in Fig. 6a, the data are fitted well into two different thermal regions. Activation energy at different concentrations of $MgBr_2$ was obtained using fitting of Eq. (6). The activation

Table 1 Extracted parameters of TGA, electrical and optical measurements for $(PVPS)_{1-x'}(MgBr_2)_{x'}$ films.

$MgBr_2$ x' (wt.%)	Thermal parameters		Electrical parameters		Optical parameters	
	T_p, °C	E_a kJ/mol	s	Activation energy (eV)	E_g (eV)	λ_{max} (nm)
				Region I		
0	333.4	133	0.30	0.38	1.2	918
10	244.4	159	0.16	0.33	1.82	866
20	238.5	189	0.18	1.13	1.9	864
30	218.5	178	0.07	1.10	2.3	894

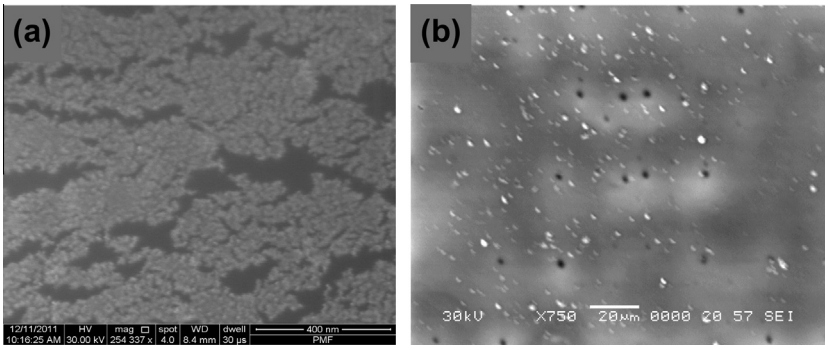

Fig. 4 SEM micrographs of $(PVPS)_{1-x'}(MgBr_2)_{x'}$ polymer composites for ($x' = 0$ and 10 wt.%).

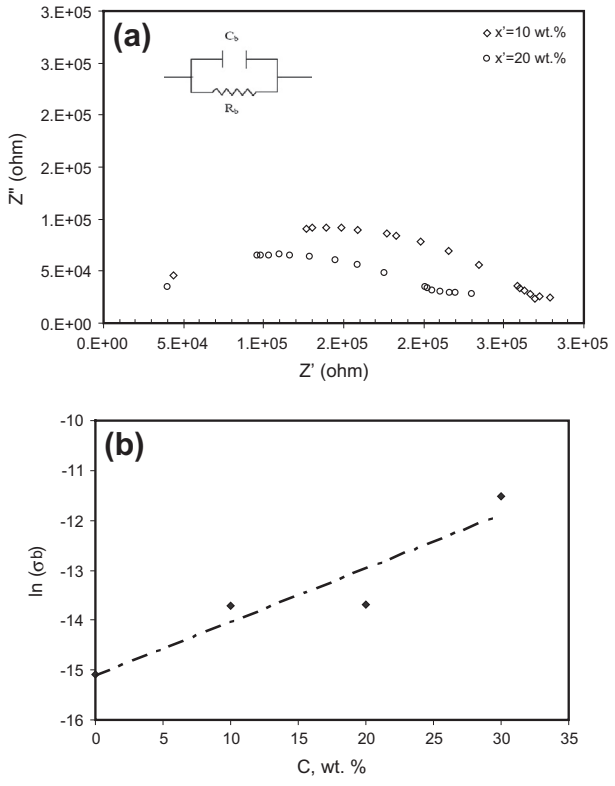

Fig. 5 (a) Cole–Cole plot for $(PVPS)_{1-x'}(MgBr_2)_{x'}$ polymer composites at $T = 303$ K and (b) Bulk conductivity of $(PVPS)_{1-x'}(MgBr_2)_{x'}$ polymer composites against $MgBr_2$ concentration.

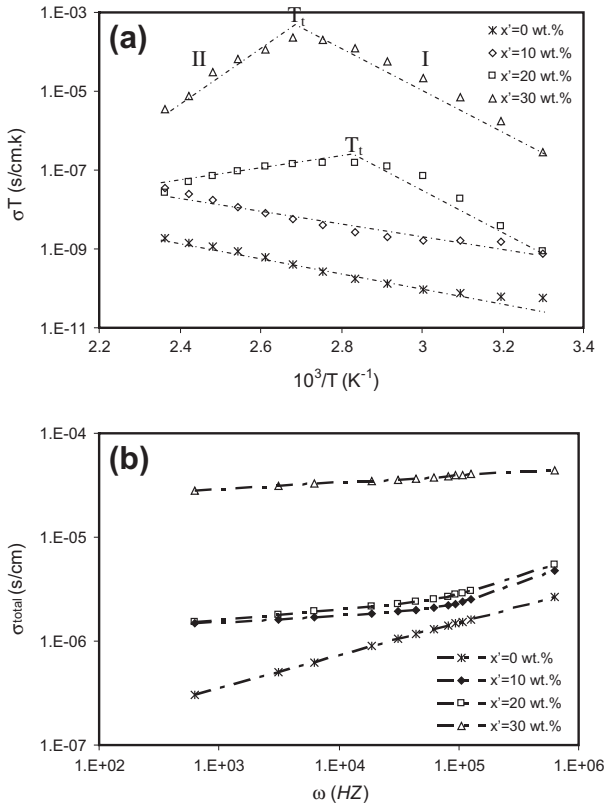

Fig. 6 (a) Temperature dependence of conductivity and (b) frequency dependence of total conductivity; for $(PVPS)_{1-x'}(MgBr_2)_{x'}$ polymer composites.

energy data are shown in Table 1. The increase in conductivity with temperature has been explained in terms of the free volume model [27]. When the temperature increases, the polymer can expand easily and then produce free volume (i.e., when the temperature increase, the free volume increase) [27]. When the free volume increased the mobility of ions increased leading to increase in the conductivity. The activation energy for 0 and 10 wt.% are equal to 0.38 and 0.33 eV (nearly unchanged) whereas its value for higher concentrations of $MgBr_2$ 20 and 30 wt.%, illustrates bigger increase 1.18 and 1.1 eV for 20 and 30 wt.% which reflects the significant effect of inorganic nanoparticles of $MgBr_2$ in the structure network. The remarkable increase of conductivity with bigger activation energy can be explained as follows. The increase of salt concentration leads to an increase of both ionic and protonic components contributing in the conductivity. Whereas the addition of the inorganic $MgBr_2$ to the polymer matrix may suppress the composite structure relaxation (it reduces ionic diffusion through structure network and subsequently charge carriers mobility). In addition the conductivity attenuation can be mainly attributed to the decrease of protonic contribution in conductivity due to water dehydration. Therefore, the competition of the activated part (mobility activation, region 1) and the decreasing of protonic component in conductivity results in the observed turnover in conductivity.

Fig. 6b shows the frequency dependence of the total conductivity of $(PVPS)_{1-x'}(MgBr_2)_{x'}$ polymer composite at 303 K, The behavior follows a universal power law [28],

$$\sigma_{ac}(\omega) = \sigma_{dc} + A\omega^{S} \quad (7)$$

where σ_{dc} is the dc conductivity (the extrapolation of the plateau region to zero frequency), A is frequency independent pre-exponential factor, ω is the angular frequency and s is the frequency exponent. In addition the relation of σ_{total} against frequency shifts upward with increasing $MgBr_2$ fractions and the kink shifts toward higher frequency range due to the domination of ionic conductivity in the polymer electrolyte. The values of the exponent s have been obtained using the least square fitting and listed in Table 1. The values of s for $(PVPS)_{1-x'}(MgBr_2)_{x'}$ films lie in the range $0 < s < 0.3$ which s decreases with increasing $MgBr_2$ concentrations.

Fig. 7a and b shows the variation of the dielectric permittivity ε' and dielectric loss ε'', for $(PVPS)_{1-x'}(MgBr_2)_{x'}$ polymer composite versus frequency at room temperature, 303 K. The figure show that ε' and ε'' a gradually decrease with increasing frequency for all prepared samples. The decrease of ε' and ε'' with frequency can be associated to the inability of dipoles to rotate rapidly leading to a lag between frequency of oscillating dipole and that of applied field. The variation indicates that at low frequencies the dielectric constant is high due to the interfacial polarization and the dielectric loss (ε'') becomes very large at lower frequencies due to free charge motion within the material [29]. This behavior can be described by the Debye dispersion relation [30],

$$\varepsilon' \cong \varepsilon_\infty + \frac{\varepsilon_s - \varepsilon_\infty}{1+\omega^2\tau^2}, \quad \varepsilon'' \cong \frac{(\varepsilon_s - \varepsilon_\infty)\omega\tau}{1+\omega^2\tau^2} \quad (8)$$

where ε_∞ and ε_s are the static and infinite dielectric permittivity, τ is the relaxation time and ω is the angular frequency.

Fig. 8a and b shows the variation of ε' and dielectric loss ε'' for $(PVPS)_{1-x'}(MgBr_2)_{x'}$ polymer composite with temperature at 1 kHz. The value of ε' and ε'' increases with temperature and then decreases at (x' = 20 and 30 wt.%), but it was increases with temperature and then fixed at (x' = 0 and 10 wt.%). At lower temperature in the dielectric constant, as the dipoles are rigidly fixed in the dielectric, the field cannot change the condition of dipoles. As the temperature increases, the dipoles comparatively become free and they respond to the applied electric field. Thus polarization increased and hence dielectric constant is also increased with the increase of temperature [31], but The dielectric loss increase with temperature, particularly at which dielectric loss due to chain motion of polymers are more effective. However, the dielectric loss is decreased with increasing temperature because the orientation polarization due to chain motion of polymer cannot keep phase with the rapidly oscillating atoms.

The optical band gap is one of the most optical parameters that explain the optical transitions. It could be defined as the difference between the bottom of the conduction band and the top of the valence band. The fundamental absorption, which corresponds to the electron excitation from the valance band to the conduction band, can be used to determine the nature and value of the optical band gap. In the present study, the optical band gap in the visible range can be estimated from the following relationship [32]

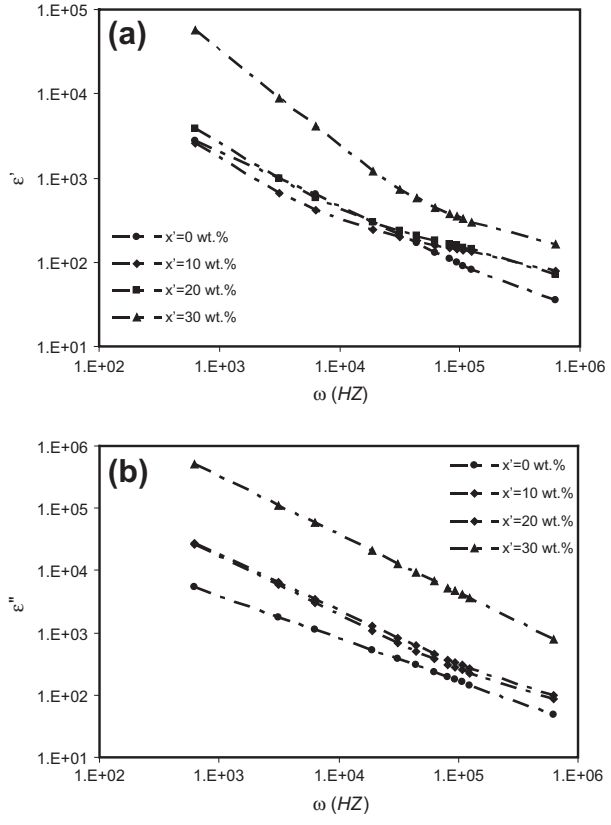

Fig. 7 Frequency dependence of (a) Dielectric constant ε', and (b) dielectric loss ε'' for $(PVPS)_{1-x'}(MgBr_2)_{x'}$ polymer composites at room temperature, 303 K.

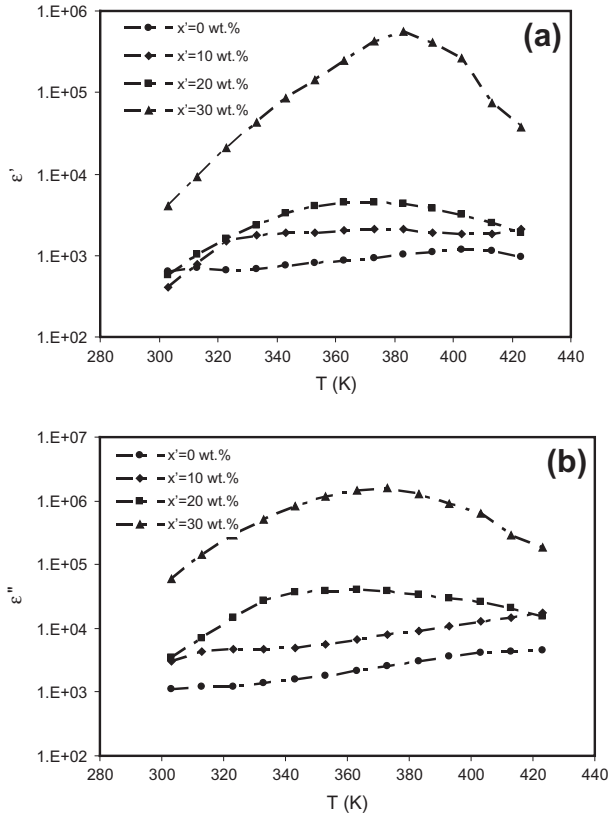

Fig. 8 Temperature dependence of (a) Dielectric constant ε', and (b) dielectric loss ε''; for $(PVPS)_{1-x'}(MgBr_2)_{x'}$ polymer composites at 1 kHz.

$$\alpha(\upsilon)h\upsilon = A'(h\upsilon - E_g)^n \quad (9)$$

where α is the absorption coefficient, υ is the frequency, h is the Planck's constant, A' is a constant, E_g is the optical energy band gap between the valence and the conduction bands and n is the power that characterizes the transition process. Fig. 9 illustrate the plot of the optical absorption against wavelength in the UV–visible range for $(PVPS)_{1-x'}(MgBr_2)_{x'}$ polymer composite in the colloidal forms. The optical absorption of $(PVPS)_{1-x'}(MgBr_2)_{x'}$ illustrates, in general, one diffused absorption peaks, their position has been determined by smoothing of absorbance-wavelength relationship, peaks position are listed in Table 1. Upon the above consideration, the maximum wavelength (λ_{max}) is decreased from 918 to 894 nm, which means that the absorption peaks make a blue shift by increasing $MgBr_2$ concentration, which may be attributed to the interaction between $MgBr_2$ and conjugate bonds in PVA. This is due to energy confinement as a result of $MgBr_2$ particle surrounded with polymer which acts as core–shell (nanoparticle-polymer core shell).

The type of transition has been tested by estimating the power n which predicts direct allowed transition from which the direct optical band gap E_g is obtained by the least square fitting of Eq. (9) for colloidal films and listed in Table 1. It is evident that the direct band gap E_g values are increased from 1.2 to 2.3 eV, so high energy is required to eject the electron from valance to conduction band. This behavior can be understood on the decrease of polymer shell thickness to the nanosize which results in the increase energy confinement. The reduction of polymer shell thickness will enhance absorption.

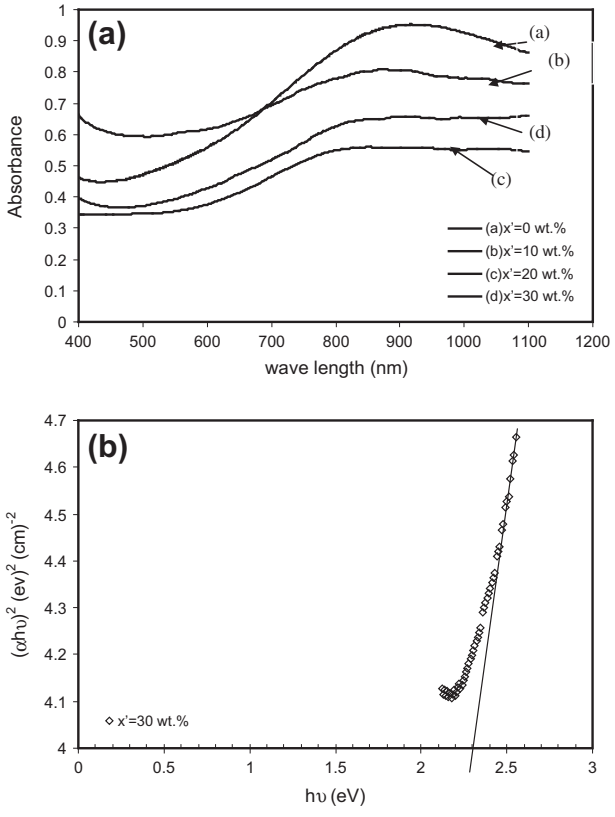

Fig. 9 (a) UV–Vis optical absorption versus wavelength and (b) plot of $(\alpha h\nu)^2$ versus $h\nu$ (eV) for $(PVPS)_{1-x'}(MgBr_2)_{x'}$ polymer composites.

In addition the decrease of the area under absorption curve with increasing salt concentration may be attributed to the light scattering.

Conclusions

We have succeeded to increase the ionic conductivity of PVPS polymer electrolyte to be 9.8×10^{-6} S/cm by adding 30 wt.% $MgBr_2$. Improving the ionic conductivity by adding $MgBr_2$ is attributed to decrease in the degree of crystallinity and increase in the charge carrier. The marked improvement of the electrical conductivity with increasing content of doping salt makes it possible to consider this electrolyte system as a potential candidate for electrochemical device applications.

Conflict of interest

The authors have declared no conflict of interest.

Compliance with Ethics Requirements

This article does not contain any studies with human or animal subjects.

Acknowledgment

M.N. would like to express her thanks for the M Sc scholarship provided by the Academy of Scientific Research and Technology Egypt Grant No: ASRT/TRG/E/2010-2.

References

[1] Armand MD. Polymer electrolytes. Annu Rev Mater Sci 1986;16:245–61.
[2] Büchi FN, Inaba M, Schmidt TJ. Chemical degradation of perfluorinated sulfonic acid membranes. polymer electrolyte fuel cell durability. New York: Springer; 2009.
[3] Staiti P, Lufrano F. Investigation of polymer electrolyte hybrid supercapacitor based on manganese oxide–carbon electrodes. Electrochim Acta 2010;55:7436–42.
[4] Granqvist CG. Handbook of inorg electrochromic mater. Amsterdam: Elsevier; 1995.
[5] Smith GB, Granqvist CG. Green nanotechnology: solutions for sustainability and energy in the built environment. Boca Raton: CRC Press; 2010.
[6] Rudhziah S, Mohamed NS, Ahmad A. Conductivity and structural studies of poly(vinylidene fluoride co-hexafluoropropylene)/polyethyl methacrylate blend doped with ammonium triflate. Int J Electrochem Sci 2013;8:421–34.
[7] Buraidah MH, Teo LP, Majid SR, Arof AK. Ionic conductivity by correlated barrier hopping in NH_4I doped chitosan solid electrolyte. Physica B 2009;404:1373–9.
[8] Fromageau J, Brusseau E, Vray D, Gimenez G, Delachartre P. Characterization of PVA cryogel for intravascular ultrasound elasticity imaging. IEEE Trans Ultrason Ferroelectr Freq Control 2003;50(10):1318–24.
[9] Kirchmeyer S, Reuter K. Scientific importance, properties and growing applications of poly(3,4-ethylenedioxythiophene). J Mater Chem 2005;15:2077–88.
[10] Groenendaal LB, Jonas F, Freitag D, Pielartzik H, Reynolds JR. Poly(3,4-ethylenedioxythiophene) and its derivatives: past, present, and future. Adv Mater 2000;12:481–94.

[11] Huang J, Miller PF, de Mello JC, de Mello AJ, Bradley DDC. Influence of thermal treatment on the conductivity and morphology of PEDOT/PSS films. Synth Met 2003;139:569–72.
[12] MacDiarmid AG. A novel role for organic polymers (nobel lecture). Synth Met 2001;40:2581–90.
[13] Hohnholz D, Okuzaki H, MacDiarmid AG. Plastic electronic devices through line patterning of conducting polymers. Adv Funct Mater 2005;15:51–6.
[14] Yan H, Endo S, Hara Y, Okuzaki H. Plastic Shottky barriers fabricated by a line patterning technology. Chem Lett 2007;36:986–7.
[15] Ouyang J, Chen CW, Chen FC, Xu Q, Yang Y. High – conductivity poly(3,4-Etylenedioxythiophene):poly(styrenesulfonate) films and its application in polymer optoelectronic devices. Adv Funct Matter 2005;15(2):203–8.
[16] Kima Y, Lee J, Kang H, Kim G, Kim N, Lee K. Controlled electro-spray deposition of highly conductive PEDOT:PSS films. Sol Energy Mater Sol Cells 2012;98:39–45.
[17] Richardson-Burns SM, Hendricks JL, Foster B, Povlich LK, Kim D, Martin DC. Controlled electro-spray deposition of highly conductive PEDOT:PSS films. Biomaterials 2007;28:1539–52.
[18] Svirskis D, Travas-Sejdic J, Rodgers A, Garg S. Electrochemically controlled drug delivery based on intrinsically conducting polymers. J Control Release 2010;146:6–15.
[19] Hu Z, Zhang J, Zhu Y. Effects of solvent-treated PEDOT:PSS on organic photovoltaic devices. Renew Energy 2014;62:100.
[20] Kim JY, Jung JH, Lee DE, Joo J. Enhancement of electrical conductivity of poly(3,4-ethylenedioxythiophene)/poly(4-styrenesulfonate) by a change of solvents. Synth Met 2002;126(2–3):311–6.
[21] Jönsson SKM, Birgerson J, Crispin X, Greczynski G, Osikowicz W, Fahlman M, et al. The effects of solvents on the morphology and sheet resistance in poly(3,4-ethylenedioxythiophene)–polystyrenesulfonic acid (PEDOT–PSS) films. Synth Met 2003;139(1):1–10.
[22] Ouyang J, Chu CW, Chen FC, Xu Q, Yang Y. High-conductivity poly(3,4-ethylenedioxythiophene):poly(styrene sulfonate) film and its application in polymer optoelectronic devices. Adv Func Mat 2005;15(2):203–8.
[23] Crispin X, Marciniak S, Osikowicz W, Zotti G, Louwet F, Fahlman M, et al. Conductivity, morphology, interfacial chemistry and stability of poly(3,4-ethylene dioxythiophene)—poly(styrene sulfonate): A photoelectron spectroscopy study. J Polym Sci B 2003;41:2561–83.
[24] Sheha E, Nasr M, El-Mansy MK. Characterization of PVA/PEDOT:PSS polymer blend: structure, optical absorption, electrical and dielectric properties. Phys Scr 2013;88(3):035701. http://dx.doi.org/10.1088/0031-8949/88/03/035701.
[25] Rao TR, Omkaram I, Veera KB, Raju Ch. Role of copper content on EPR, susceptibility and optical studies in poly(vinylalcohol) (PVA) complexed poly(ethyleneglycol) (PEG) polymer films. J Mol Struct 2013;1036:94–101.
[26] Kwei TK. The effect of hydrogen bonding on the glass transition temperatures of polymer mixtures. J Polym Sci Polym Lett 1984;22:307.
[27] Polu AR, Kumar R. Ionic Conductivity And Electrochemical Cell Studies Of New Mg2+ ion Conducting PVA/PEG Based Polymer Blend Electrolytes. Adv Mat Lett 2013;4(7):543–7.
[28] Gupta PN, Singh KP. Characterization of H_3PO_4 based PVA complex system. Solid State Ionics 1996;86–88(1):319–23.
[29] Kyritsis A, Pissis P, Grammatikakis J. Dielectric relaxation spectroscopy in poly(hydroxyethyl acrylates)/water hydrogels. J Polym Sci, Part B: Polym Phys 1995;33(12):1737–50.
[30] Nora E. Dielectric properties and molecular behavior. London: Van Nostrand; 1969.
[31] Frohlick H. Theory of dielectrics. Oxford University Press; 1956, p. 13.
[32] Jestl M, Maran I, Kock A, Beinsting W, Gornik E. Polarization-sensitive surface plasmon Schottky detectors. Opt Lett 1989;14:719–21.